CrystEngComm

Luminescent polymorphic crystals: mechanoresponsive and multicolor-emissive properties

Journal:	*CrystEngComm*
Manuscript ID	CE-HIG-12-2021-001614.R1
Article Type:	Highlight
Date Submitted by the Author:	30-Dec-2021
Complete List of Authors:	Ito, Suguru; Yokohama National University, Department of Chemistry and Life Science, Graduate School of Engineering Science; Japan Science and Technology Agency, PRESTO

HIGHLIGHT

Luminescent polymorphic crystals: mechanoresponsive and multicolor-emissive properties

Suguru Ito*[a,b]

Received 00th January 20xx,
Accepted 00th January 20xx

DOI: 10.1039/x0xx00000x

Mechanoresponsive luminescent organic crystals have recently attracted increasing interest owing to their potential applications in advanced optoelectronic devices, mechanosensors, security technologies, etc. In the past few years, an increasing number of polymorphic organic crystals have emerged to elucidate the relationship between the crystal structure and mechanoresponsive properties of luminescent organic crystals. This highlight article will introduce the recent progress in luminescent organic polymorphs with mechanoresponsive properties. Multicolor emission and multistimuli-responsive switching of fluorescence have been achieved for various polymorphic organic crystals that exhibit mechanochromic luminescence (MCL). Remarkable studies have also been carried out for the development of polymorphic MCL crystals showing different thermally activated delayed fluorescence (TADF) and room-temperature phosphorescence (RTP) properties depending on their crystal structures. In addition to the formation of polymorphs, the crystallization of pseudopolymorphs and cocrystals is also effective in controlling the luminescence and MCL properties of organic luminescent compounds. Moreover, polymorphic crystals that exhibit other mechanoresponsive behaviors, such as mechanoluminescence (ML), have been highlighted. Based on the deep insights into the luminescence properties and mechanoresponsive behaviors of polymorphic crystals, further research is expected to establish rational guidelines for the prediction and creation of organic crystals with desired photophysical and mechanical properties.

1. Introduction

Luminescent organic crystals have attracted considerable interest in the past decade. Although concentration quenching has long been an obstacle to efficient luminescence in the solid state, an increasing number of organic molecules that are highly luminescent in the crystalline state has been created based on appropriate molecular design strategies.[1–4] In addition to organic fluorophores that exhibit prompt fluorescence (PF) from the singlet excited state S_1 to the ground state S_0, a growing number of organic emitters showing thermally activated delayed fluorescence (TADF)[5–7] or room-temperature phosphorescence (RTP)[8–10] have been developed and crystallized as luminescent organic crystals (Fig. 1). Phosphorescence is a radiative transition from a triplet excited state T_1 to S_0. The T_1 state is produced from S_1 through intersystem crossing (ISC). The mechanism of TADF is based on the up-conversion from T_1 to S_1 through reverse intersystem crossing (RISC). Small energy splitting (ΔE_{ST}) between S_1 and T_1 states is required to achieve efficient TADF emission.

Polymorphic crystals, in which identical molecules are arranged in different packing structures in crystallization, have different physical properties such as melting point and solubility.[11–13] The physical properties of crystals are also changed by the formation of pseudopolymorphic crystals, which have different packing structures by the inclusion of solvent molecules.[14,15] Controlling the formation of polymorphs is an important issue in the field of the pharmaceutical industry.[16,17] Since the luminescent properties of organic crystals are governed by the molecular structures and packing modes, the control of polymorphism is also important in luminescent organic crystals.[18] In other words, the emission color is tunable by creating polymorphic crystals from the same molecule. Meanwhile, the luminescent properties of an organic molecule in its crystalline state are difficult to predict and control, and therefore the further studies on luminescent polymorphs are indispensable to establish the design guidelines of luminescent organic crystals.

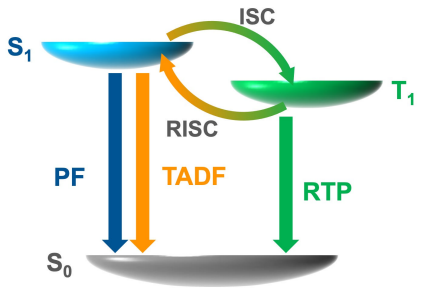

Fig. 1 Energy diagram for prompt fluorescence (PF), thermally activated delayed fluorescence (TADF), and room-temperature phosphorescence (RTP).

[a] *Department of Chemistry and Life Science, Graduate School of Engineering Science, Yokohama National University, 79-5 Tokiwadai, Hodogaya-ku, Yokohama 240-8501, Japan. E-mail: suguru-ito@ynu.ac.jp*
[b] *PRESTO, Japan Science and Technology Agency (JST), 4-1-8 Honcho, Kawaguchi, Saitama 332-0012, Japan.*

Another important challenge in the field of luminescent organic crystals is the development of stimuli-responsive crystals that can switch luminescence properties.[19–21] Since mechanical stimulation is the ubiquitous external stimulus, mechanoresponsive organic crystals have been intensively investigated in recent years.[22] Mechanochromic luminescence (MCL) is attracting particularly large attention.[23–25] The MCL crystals switch their luminescence colors in response to external mechanical stimuli such as grinding, shearing, and pressure. Typically, the emission-color change is attributed to the amorphization of the crystals. The original emission color is generally recovered by the recrystallization of the amorphous state into the initial crystals upon heating or exposure to solvent vapors. The MCL materials have potential applications in pressure sensors, security inks, wearable devices, etc.

Polymorphic and pseudopolymorphic organic crystals can switch their luminescence properties by interconversion or conversion to amorphous solids in response to external stimuli (Fig. 2).[26–31] Their responsiveness to external stimuli depends on the molecular arrangements in the packing structure.[32] Detailed analysis of the structure and stimuli-responsive properties of organic crystals will lead to the establishment of new design guidelines for stimuli-responsive luminescent crystals. Over the past few years, there has been a rapid increase in the number of papers on the mechanical-stimuli-responsive organic polymorphic and pseudopolymorphic crystals. It appears timely to highlight these emerging research topics.

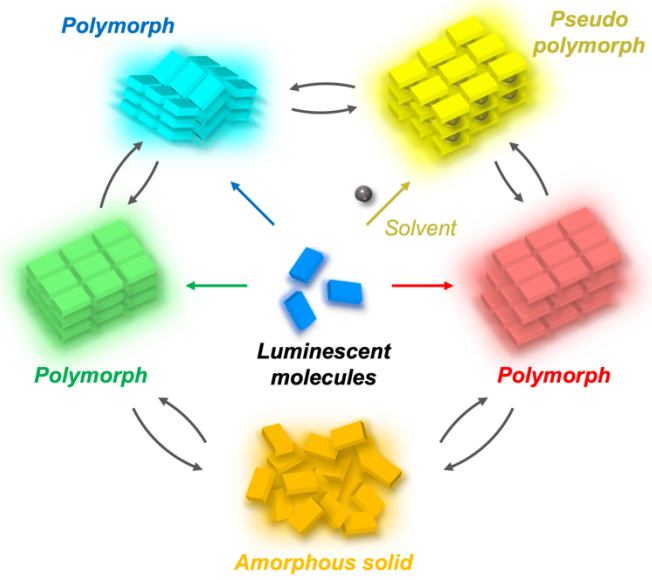

Fig. 2 Schematic representation of the polymorph- and pseudopolymorph-dependent luminescence and stimuli-responsive switching of organic crystals.

The recent reviews from Yan and coworkers published in 2014 and 2019 have focused on the control of luminescence properties by polymorphs and the photofunctional polymorphs, respectively.[18,33] This highlight summarizes recent examples (since 2018) on the mechanoresponsive behaviors of luminescent organic polymorphs. Luminescent polymorphs of organometallic complexes are outside the scope of this highlight. In Sections 2 and 3, typical MCL and multicolor MCL of fluorescent polymorphs have been introduced. The effects of crystal structure on TADF and RTP properties have been discussed in Section 4. Furthermore, the control of MCL by forming pseudopolymorphic crystals and cocrystals has been described in Section 5. Mechanoresponsive properties other than MCL exhibited by polymorphic crystals have also been presented in Section 6. Finally, a summary and perspectives for the mechanoresponsive luminescent polymorphs have been described in Section 7.

2. Mechanochromic luminescence (MCL) of fluorescent organic polymorphs

2.1. Polymorphic tetraphenylethene (TPE) derivatives

Tetraphenylethene (TPE) is a representative compound with aggregation-induced emission (AIE) properties and generally exhibits efficient fluorescence in the solid state.[34] Several fluorescent organic crystals of substituted TPE derivatives have been developed to show MCL.[35–38]

As a recent example of polymorphic MCL by a TPE derivative, Cui, Yang, and coworkers reported TPE-dioxaborine derivative **1** in 2020 (Fig. 3a).[39] The four polymorphs and one amorphous state of **1** showed green, yellow, orange, and red emission colors with high fluorescence quantum yields of 41–74%. Intense green emission was observed for orthorhombic crystals **1-G** (*Pbcn*) and monoclinic crystals **1-G'** (*P*2/*c*). The green-emissive crystals exhibited centrosymmetric π-stacked dimers between the adjacent molecules. Orange-emissive tetragonal crystals **1-O** ($P4_32_12$) also exhibited dimers, albeit rotationally symmetric structures. In contrast, molecules in yellow-emissive orthorhombic crystals **1-Y** ($Pca2_1$) presented lamellar arrangements without dimeric structures. Notably, the emission wavelength of **1-G** and **1-G'** exhibiting dimer structures were observed in the hypsochromic region compared with that of **1-Y** having no significant π-interaction, which was rationalized in terms of the efficient stabilization of HOMO in the dimers of **1-G**. All crystalline samples changed to red-emissive amorphous state **1-R** upon grinding. The ground **1-R** changed to yellow-emissive **1-Y** in response to heating or exposure to dichloromethane vapor. Moreover, **1-G**, **1-G'**, and **1-O** also transformed into **1-Y** upon heating or fuming. These results indicate that **1-Y** is the most thermodynamically stable crystal.

Feng, Zou, Tang, and coworkers also reported the mechanoresponsive properties of pyridinium-substituted TPE derivative **2** in 2021 (Fig. 3b).[40] Based on the molecular conformation and luminescent properties of three polymorphs of **2**, the mechanoresponsive bathochromic shifts of the emission wavelength could be explained by the planarization of the molecular conformation.

2.2. Polymorphs of triphenylamine (TPA)-based D-A compounds

Crystals of donor-acceptor (D-A)-type compounds often exhibit MCL since the emission color of D-A-type fluorophores is

sensitive to the polarity of their surrounding environments. Triphenylamine (TPA) group is widely used as donor unit of D-A-type fluorophores, and TPA-based D-A compounds frequently show solid-state emission in the crystalline state.[4] The steric bulk of the TPA unit is effective to reduce the concentration quenching by intermolecular interactions in the crystals of D-A-type fluorophores.

Moon, Anthony, and coworkers have been reported several TPA-based fluorophores that exhibit MCL properties.[41–43] They recently reported different mechanoresponsive behaviors of two polymorphic crystals of a new fluorophore **3** composed of TPA donor and Meldrum's acid acceptor (Fig. 3c).[44] Both yellow-emissive **3-Y** and red-emissive **3-R** with space groups of $P2_1/c$ and P-1, respectively, were obtained from a CH_2Cl_2-hexane mixture. The emission intensity of **3-Y** was reduced upon hard crushing and recovered by heating at 130 °C. Hard crushing of **3-R** also resulted in the reduction of the emission intensity. Notably, the ground **3-Y** changed to yellow- and orange-emissive states when heated at 180 and 80 °C, respectively.

In 2021, Cao, Zhang, and coworkers reported the red to near-infrared (NIR) MCL of TPA-substituted benzothiadiazole **4** containing acrylonitrile group (Fig. 3d).[45] Two polymorphic crystals **4-R** ($P2_1/c$) and **4-N** (P-1) were obtained from a dichloromethane/hexane mixed solution of **4** and showed red and NIR emission at 615 and 727 nm, respectively. In response to grinding stimuli, the fluorescence maximum of **4-R** changed to 775 nm. The emission color of **4-N** was almost unchanged by hand-actuated grinding but shifted to 773 nm by machine-actuated grinding. A high degree of molecular coplanarity around the benzothiadiazole and the adjacent benzene and acrylonitrile groups should account for the NIR emission from the ground **4-R**.

In the same year, Ishi-i and coworkers realized the multicolor fluorescence switching of TPA-based benzothiadiazole derivatives **5a–d** (Fig. 3e).[46] Three out of four derivatives formed polymorphic crystals that exhibited different emission colors. Especially, *m*-formyl-substituted **5b** was crystalized as three polymorphs **5b-Y**, **5b-yO**, and **5b-rO** that exhibited yellow, yellowish-orange, and reddish-orange

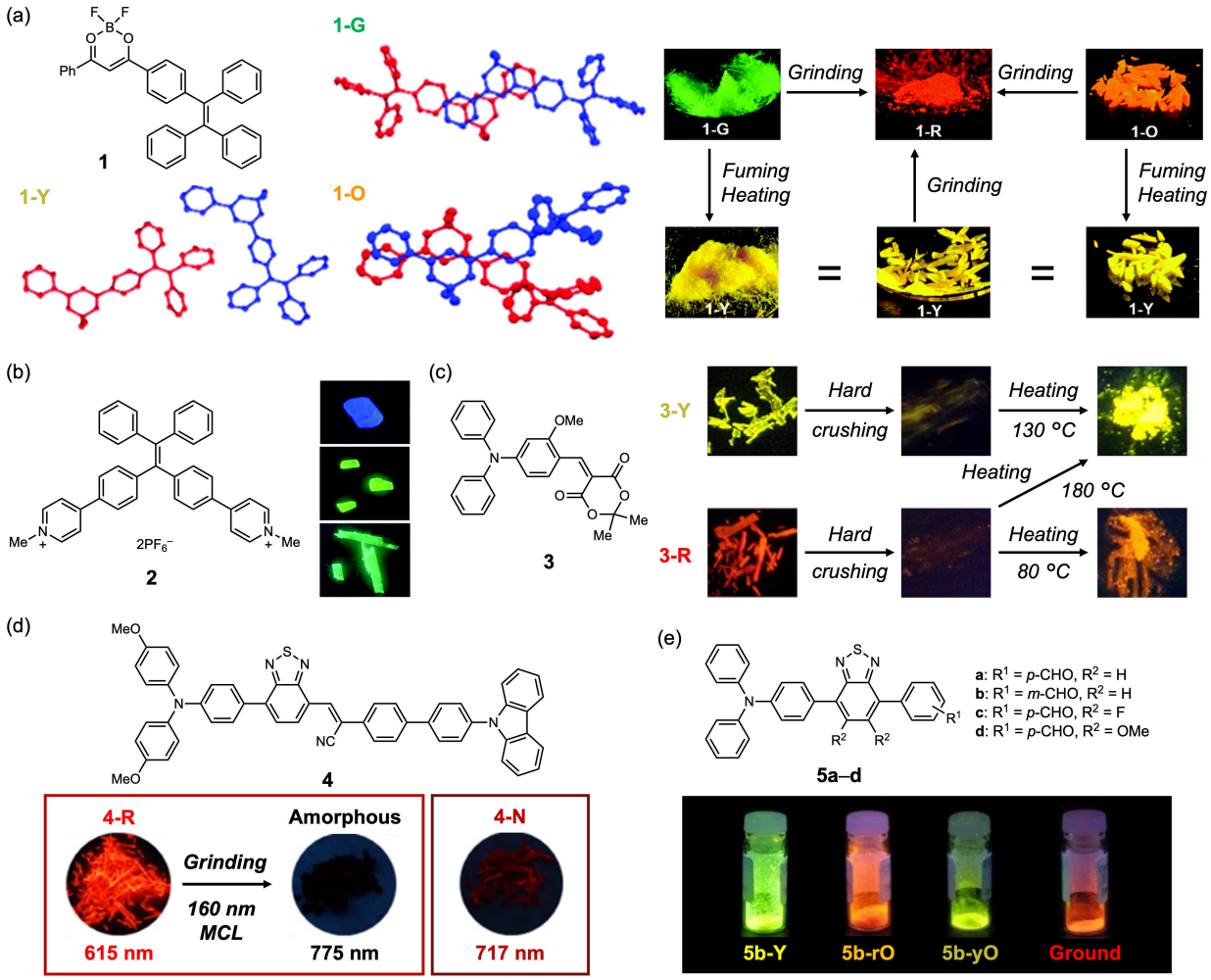

Fig. 3 Polymorph-dependent fluorescence and MCL of TPE derivatives (a) **1** and (b) **2** and TPA derivatives (c) **3**, (d) **4**, and (e) **5**. (a and b) Reproduced from Refs. 39 and 40 with permission. Copyright 2020 and 2021 Royal Society of Chemistry. (c) Reproduced from Ref. 44 with permission. Copyright 2018 American Chemical Society. (d and e) Reproduced from Refs. 45 and 46 with permission. Copyright 2021 Wiley-VCH Verlag GmbH & Co. KGaA, Weinheim.

fluorescence, respectively. Upon grinding, the emission color of the three polymorphs changed to red. The ground state changed into **5b-yO** by fuming. Moreover, **5b-Y** and **5b-rO** were transformed into **5b-yO** after being heated. Detailed structural analyses of the polymorphs suggested that the continuous internal space in the metastable polymorph should be the origin of the large shift in the MCL.

2.3. Benzothiadiazole-based D-A compounds

Not limited to the combination with TPA, the benzothiadiazole unit has been utilized as an efficient electron-accepting unit to produce various D-A-type fluorophores that exhibit versatile MCL properties in the crystalline state. For example, Ito and coworkers have been reported the self-recovering MCL and two-step MCL of benzothiadiazole-based D-A-type fluorophores.[47–50] In the case of D-A-type benzothiadiazoles containing triphenylimidazole unit as a donor moiety, the MCL properties were changed significantly between morphologically different crystals, which could be obtained by the slight modification of the steric bulk of the substituent.[51]

Multi-color MCL of three polymorphic crystals was achieved by a thienyl-substituted benzothiadiazole derivative **6** in 2021 (Fig. 4).[52] The green-emissive triclinic (*P*-1) crystal **6-G** showed typical MCL between the green-emissive crystal and a yellow-emissive amorphous state. The yellow-emissive monoclinic ($P2_1/n$) crystal **6-Y**, containing disordered solvent molecules, was transformed into an orange-emissive amorphous state upon grinding. When **6-Y** was heated to 150 °C, another solvate-free $P2_1/c$ crystal **6-YO** showing yellowish orange emission was obtained. The emission color of **6-YO** was changed to orange upon amorphization by grinding.

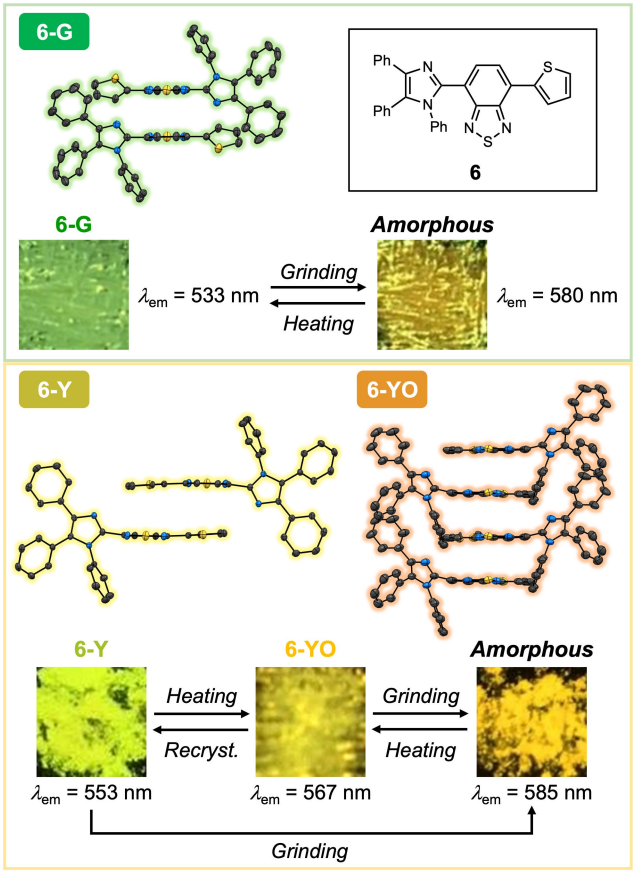

Fig. 4 Bicolor MCL of green-emissive polymorph **6-G** (top) and tricolor MCL of yellow-emissive and yellow-orange emissive polymorphs **6-Y** and **6-YO** (bottom). Reproduced from Ref. 52 with permission. Copyright 2021 Royal Society of Chemistry.

2.4. Miscellaneous examples of recent polymorphic MCL crystals

Cyanostilbene derivatives reported by Park and coworkers in 2002 are one of the most representative fluorophores that exhibits aggregation-induced enhanced emission (AIEE).[53] A considerable number of cyanostilbene derivatives have been developed to show MCL.[54] As a recent example of polymorphism-dependent MCL of cyanostilbene derivatives, Yang and coworkers reported a diarylphosphanyl-substituted stilbene derivative **7** in 2018 (Fig. 5a).[55] Yellow- and orange-emissive polymorphs **7-Y** and **7-O** with space groups of *P*-1 and $P2_1/c$, respectively, changed to yellow-orange-emissive amorphous states upon grinding. In 2020, Park and coworkers reported the tricolor fluorescence switching of a dicyanodistyrylbenzene derivative **8** having dodecyloxy side chains (Fig. 5b).[56] The polymorphic crystals **8-B** and **8-O** exhibited blue and orange fluorescence, which were changed to green-emissive states by applying a shear force.

In 2019, pyridyl-substituted fluorene **9** was developed by Yuan, Wang, and coworkers to form three polymorphic crystals with violet, blue, and green emission (Fig. 5c).[57] The emission colors of the polymorphs could be switched in response to mechanical grinding. Based on the single-crystal X-ray diffraction analyses, the violet and blue emission of $P2_12_12_1$ and *P*-1 polymorphs, respectively, should be attributed to the different dimers of **9**. Meanwhile, the origin of green emission from another $P2_12_12_1$ crystal should be the formation of supramolecular chains based on weak π-stacks of **9**. Another fluorene-based compound **10** that can form two polymorphs was reported by Ji, Huo, and coworkers in 2020 (Fig. 5d).[58] Upon grinding, the emission wavelengths of sky-blue-emissive and green-emissive polymorphs were shifted by 61 and 84 nm, respectively. The difference in emission wavelength of these polymorphs was explained by the different molecular coplanarities of **10** in the crystalline states.

Polymorphic crystals of fluorophore **11** containing a phenolic hydroxy group were reported by Huang, Wu, and coworkers in 2019 (Fig. 5e).[59] The D-π-A asymmetric 4*H*-pyran derivative **11** formed three polymorphic crystals that exhibit yellow, orange, and red fluorescence. All polymorphs were changed to orange-emissive amorphous states upon grinding. The molecular conformations and packing arrangements should determine the emission colors of yellow- and red-emissive crystals, whereas the orange emission should mainly be attributed to the planar conformation of **11** in the crystalline state.

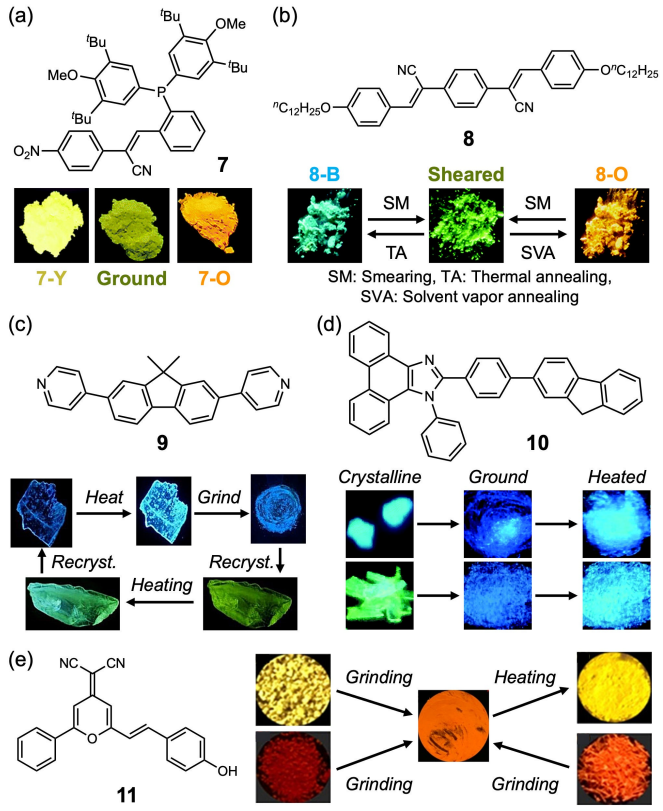

Fig. 5 Photographs of the MCL for polymorphic crystals of (a) **7**, (b) **8**, (c) **9**, (d) **10**, and (e) **11** under UV irradiation. (a, b, and d) Reproduced from Refs. 55, 56, and 58 with permission. Copyright 2018 and 2020 Royal Society of Chemistry. (c) Reproduced from Ref. 57 with permission. Copyright 2019 Wiley-VCH Verlag GmbH & Co. KGaA, Weinheim. (e) Reproduced from Ref. 59 with permission. Copyright 2019 American Chemical Society.

3. Two-step switching and acidochromism of fluorescent polymorphic MCL crystals

3.1. Two-step MCL of polymorphic organic crystals

Generally, the emission color of MCL crystals switches between two colors because the mechanism of the emission-color change in typical MCL crystals is based on the crystal-to-amorphous phase transitions induced by mechanical stimuli. Relatively few are known to exhibit two-step MCL that can change the emission color in a stepwise manner in response to mechanical stimuli of different intensities.[49,60–64] Understanding the two-step MCL of polymorphic crystals should provide profound insights into the responsiveness of organic luminescent crystals to mechanical stimuli.[29,65]

In 2019, Wang, Ge, and coworkers reported that difluoroboron complex **12** with TPE and furyl groups could form four polymorphic crystals **12-Y**, **12-R**, **12-N**, and **12-F** with different emission properties (Fig. 6a).[66] The emission wavelength of the polymorphs shifted by 11–48 nm in the hypsochromic direction upon slight grinding. Further strong grinding resulted in the bathochromic shift of the emission wavelength up to 51 nm. Tanaka, Chujo, and coworkers also reported the two-step MCL of difluoroboron complex **13** in 2020 (Fig. 6b).[67] The thienyl-substituted boron ketoiminate **13** formed two polymorphic crystals from THF and methanol solutions that exhibit green and orange emission, respectively. Only the orange-emissive crystals exhibited a two-step MCL.

Ito and coworkers reported two-types of two-step MCL of benzothiadiazole-based D-A-type fluorophores **14** in 2020 (Fig. 6c).[68] Among a series of *N*-substitutedphenyl derivatives **14**, *p*-bromo and *o*-bromo-substituted compounds exhibited one-way type and back-and-forth type two-step MCL, respectively. The first emission-color switching of the one-way type MCL was rationalized in terms of the phase transition from the initial crystal to another polymorph, and the amorphization of the crystal structures should account for the second step. Meanwhile, the destruction of extended intermolecular interactions upon crushing should cause the initial emission switching of the back-and-forth type MCL.

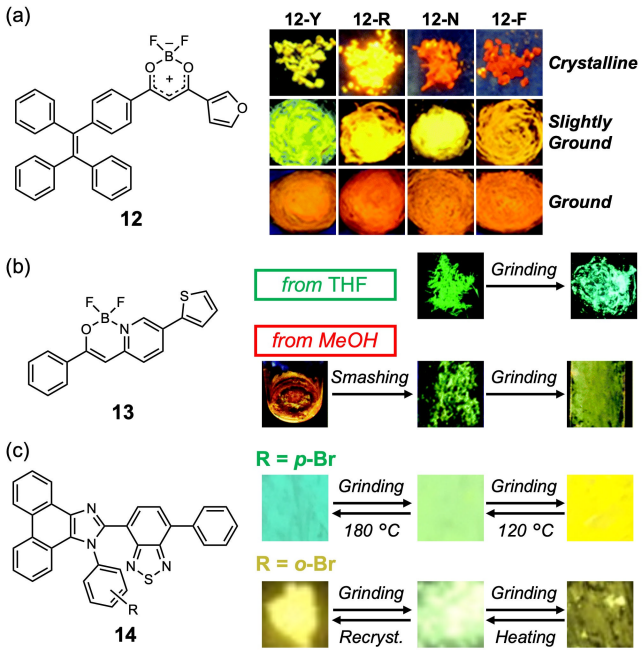

Fig. 6 Two-step MCL for the polymorphic crystals of (a) **12** and (b) **13**. (c) Two types of two-step MCL by **14**. Reproduced from Refs. 66, 67, and 68 with permission. Copyright 2019 and 2020 Royal Society of Chemistry.

3.2. Mechano- and acid-responsive fluorescence of polymorphic crystals

The solid-state fluorescence of organic compounds containing a basic moiety in their conjugated systems can be switched by exposing acid vapor. An increasing number of crystalline organic fluorophores have been reported to show both MCL and acidochromism.[69–73] Since polymorphic crystals often undergo phase transition upon heating or exposure to solvent vapors, the formation of polymorphic MCL crystals from fluorophores with an acid-responsive unit should be a rational strategy to create multi-stimuli-responsive crystals.

The introduction of the pyridyl group is a facile method to induce the acid-responsive property to organic fluorophores. Xu, Tian, and coworkers achieved multi-stimuli-responsive fluorescence switching of pyridyl-substituted styrylanthracene derivative **15** in 2019 (Fig. 7a).[74] Green-emissive triclinic crystal **15-G** (*P*-1) and orange-emissive monoclinic crystal **15-O** ($P2_1/c$) were obtained as polymorphs of **15**. The emission color of the two polymorphs shifted in the bathochromic direction upon amorphization by grinding. After heating the ground samples of both polymorphs, the emission color changed to the green of **15-G**. The emission color of both polymorphs also responded to HCl fumigation and shifted in the bathochromic direction. In 2020, Li, Sun, and coworkers also reported the acidochromism of polymorphic crystals of pyridyl-substituted anthracene derivative **16** (Fig. 7b).[75] Among four polymorphs **16-A**, **16-B**, **16-C**, and **16-D**, two polymorphs **16-B** and **16-D** exhibited typical bicolor MCL. On the other hand, the ground sample of **16-A** changed to **16-D** upon exposure to CH_2Cl_2 vapor. Upon exposure to HCl vapor, the emission wavelength of **16-A** and **16-B** were

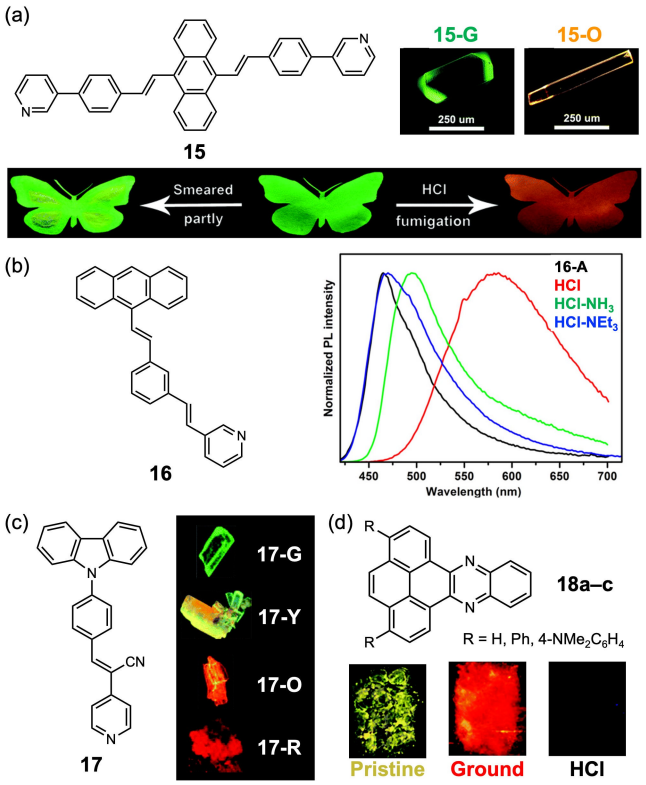

Fig. 7 (a) Photographs for the polymorph-dependent emission and mechano- and HCl-responsive switching of **15**. Reproduced from Ref. 74 with permission. Copyright 2019 Royal Society of Chemistry. (b) Fluorescence spectra for the acidochromism of **16-A**. Reproduced from Ref. 75 with permission. Copyright 2020 American Chemical Society. (c) Photographs for the polymorph-dependent emission of **17**. Reproduced from Ref. 76 with permission. Copyright 2021 Royal Society of Chemistry. (d) Photographs for the mechano- and HCl-responsive emission of the yellow-emissive polymorph of **18c**. Reproduced from Ref. 77 with permission. Copyright 2020 Royal Society of Chemistry.

significantly shifted in the bathochromic direction. When the acid-exposed samples were treated with NEt_3 vapor, both samples changed to **16-A**. Interestingly, upon exposure to NH_3 vapor, both samples were transformed into **16-C**. Moon, Anthony, and coworkers reported the MCL and acidochromism of pyridyl-substituted carbazole derivative **17** (Fig. 7c).[76] Four polymorphic crystals **17-G**, **17-Y**, **17-O**, and **17-R** exhibited green, yellow, orange, and red fluorescence, respectively. In response to mechanical or thermal stimuli, polymorphs **17-Y**, **17-O**, and **17-R** were converted to **17-G**, which should be the most stable polymorph. The emission color of **17-G** was changed to red by treating with trifluoroacetic acid (TFA) vapor, and the original green emission was recovered after exposure to NH_3 vapor.

In addition to pyridyl-substituted derivatives, crystalline fluorophores consisting of nitrogen-containing basic heteroaromatic rings exhibit acid-responsive emission-color changes. In 2020, Sutherland and coworkers reported the acid-responsive quenching of the solid-state fluorescence of quinoxaline-fused pyrene derivatives **18a–c** (Fig. 7d).[77] Among these, dimethylamino-substituted **18c** exhibited the MCL between two polymorphic crystals that exhibit yellow and red emission. The introduction of the dimethylamino groups was effective to induce the formation of J-type aggregates exhibiting yellow fluorescence.

4. Thermally activated delayed fluorescence (TADF) and room temperature phosphorescence (RTP)

4.1. Polymorph-dependent TADF and MCL

Organic emitters that exhibit thermally activated delayed fluorescence (TADF) have attracted considerable interest in the past few decades owing to the wealth of their potential applications in high-efficiency OLEDs, photodynamic therapy (PDT), and biomedical sciences.[5–7] Although intensive investigations have been carried out to elucidate the relationship between the molecular structure and TADF properties, further studies are still required to understand and control the TADF from crystals.[78–82] Moreover, TADF crystals exhibiting MCL behavior are promising as advanced multifunctional materials.[83–87] Recent studies on TADF and MCL properties of polymorphic crystals have provided some insights into the structure–property relationship of crystalline TADF emitters.

In 2018, Lee and coworkers examined a systematic tuning of TADF properties by forming different aggregation states (Fig. 8a).[88] 2-(Phenothiazine-10-yl)-anthraquinone (**19**) formed five different aggregation states including three polymorphic crystals. Two monoclinic crystals with space groups of $P2_1/n$ and $P2_1/c$ exhibited yellow (Y-crystal: λ_{em} = 554 nm) and red (R-crystal: λ_{em} = 606 nm) emission, respectively. Triclinic polymorph (*P*-1) showed orange emission (R-crystal: λ_{em} = 568 nm). Yellow- and red-emissive amorphous solids with maximum emission wavelengths of 545 nm (Y-solid) and 649 nm (R-solid), respectively, were also obtained. Typical TADF properties were observed for these aggregates except red-emissive solid. Well-

separated HOMOs and LUMOs were visualized by TD-DFT calculations of dimer or trimer models of polymorphic crystals, which should account for the small ΔE_{ST} values and TADF properties of these polymorphs.

Another example of polymorph-dependent TADF and MCL by quinoxaline-based emitters **20a** and **20b** was reported by Yang and coworkers in 2020 (Fig. 8b).[89] Greenish yellow-emissive **20a** and orange-emissive **20b** changed their emission colors to red upon grinding. The ground samples were transformed into yellow-emissive states upon exposure to CH_2Cl_2 vapor. The two emitters **20a** and **20b** formed four and five different aggregation states, respectively. All aggregates exhibited distinct TADF emissions. Regardless of the difference in the aggregated structures, fluoro-substituted **20b** showed significantly shorter lifetimes of delayed components and higher rate constants of RISC processes compared with **20a**. That is, the TADF properties were determined by the molecular structure. Meanwhile, the emission wavelength and quantum yield of TADF were controlled by the aggregated structures. In the same year, Yang and coworkers also reported the polymorph-dependent TADF and MCL of dipyridyl-substituted pyridopyrazine derivative **21** (Fig. 8c).[90] Yellow-emissive crystals **21-Y** and orange-yellow-emissive crystals **21-OY** with different TADF properties were changed to orange-emissive amorphous states **21-O** in response to mechanical stimuli. Furthermore, Yang and coworkers reported the on-off switching of polymorph-dependent TADF in 2021 (Fig. 8d).[91] Yellow-emissive states of 7*H*-benzo[*c*]phenoxazine derivative **22** exhibited only prompt luminescence on nanosecond time scales. Upon grinding, the yellow-emissive **22** changed to a red-emissive amorphous state. Polymorphic crystals of **22** also exhibited red emission. These red-emissive states exhibited long-lived delayed fluorescence. The efficient intermolecular π-stacks of **22** molecules in the red-emissive states should decrease S_1 energy level, which should account for the mechanoresponsive turn-on switching of TADF properties.

In 2021, Li and coworkers developed diquinoxalino[2,3-*a*:2′,3′-*c*]phenazine derivative **23** that can exhibit polymorph-dependent TADF and MCL (Fig. 8e).[92] The emission bands of yellow- and red-emissive polymorphs **23-Y** and **23-R** shifted in the NIR region upon grinding. The red-emissive crystals exhibited a higher proportion of delayed fluorescence than the yellow-emissive crystals. Efficient intermolecular interactions in

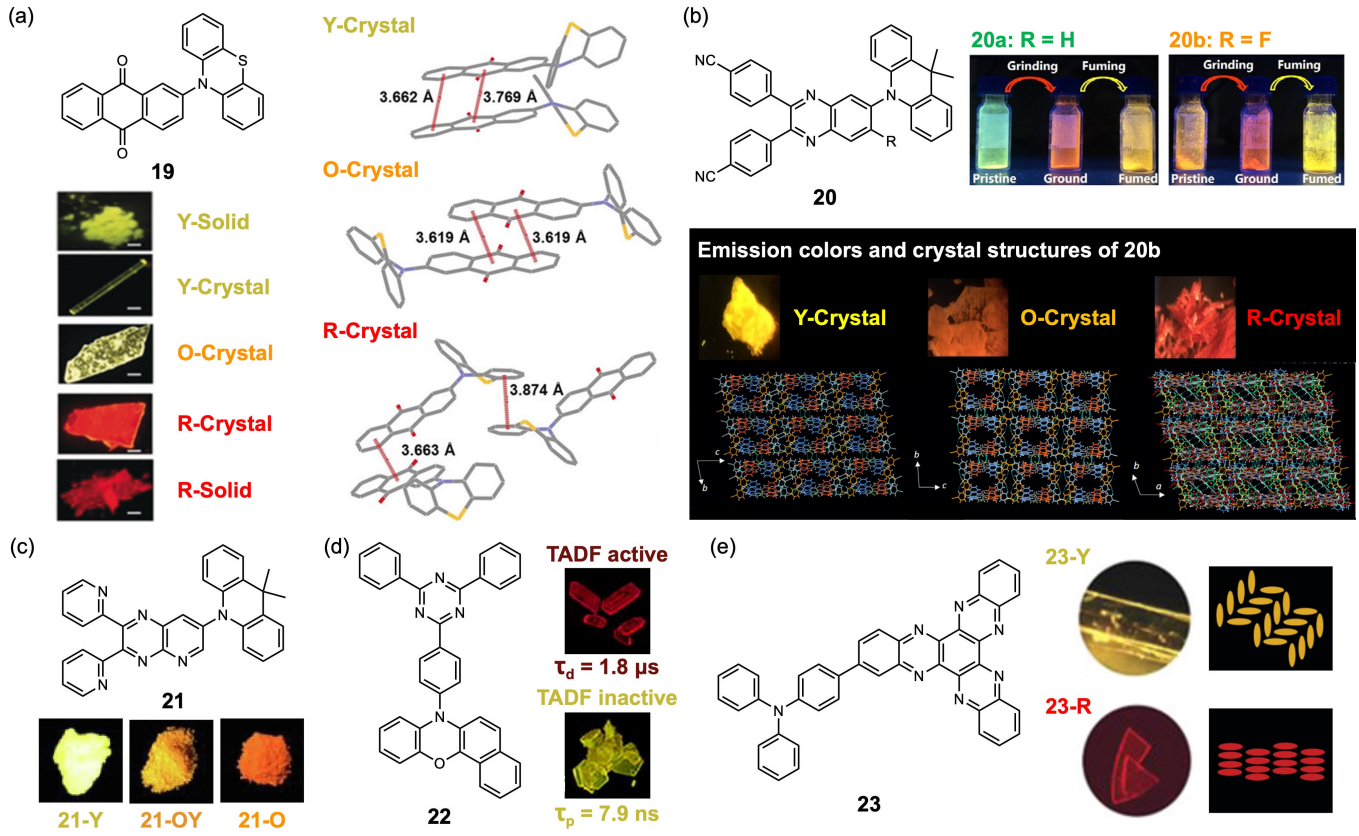

Fig. 8 (a) Photographs of five aggregation states of **19** under UV (left) and intermolecular interactions in the polymorphs of **19** (right). Reproduced from Ref. 88 with permission. Copyright 2018 Wiley-VCH Verlag GmbH & Co. KGaA, Weinheim. (b) MCL of **20a** and **20b** (top) and emission colors and crystal structures of **20b** (bottom). Reproduced from Ref. 89 with permission. Copyright 2020 Wiley-VCH Verlag GmbH & Co. KGaA, Weinheim. (c) Photographs of polymorphs and amorphous state of **21** under UV. Reproduced from Ref. 90 with permission. Copyright 2020 Elsevier. (d) Photographs of polymorphs of **22** under UV. Reproduced from Ref. 91 with permission. Copyright 2021 Elsevier. (e) Photographs under UV and packing structures of polymorphs of **23**. Reproduced from Ref. 92 with permission. Copyright 2021 Wiley-VCH Verlag GmbH & Co. KGaA, Weinheim.

the lamellar arrangement would account for the longer lifetimes of the red-emissive crystals compared with those in the yellow-emissive crystals in a herringbone structure.

4.2. Polymorph-dependent RTP and MCL

Materials that exhibit room-temperature phosphorescence (RTP) are expected to find applications in displays, emergency lights, cryptography, bio-imaging, etc. Although inorganic noble metal complexes have been widely explored as RTP materials, an increasing number of purely organic compounds exhibiting RTP have been developed recently.[93–95] At the molecular level, the introduction of carbonyl groups, heteroatoms, or heavy halogen atoms is often effective to achieve RTP by organic crystals. However, more detailed investigations are needed to reveal the effects of molecular conformations and packing structures on RTP properties. Recently, several polymorphic systems have been reported to show different RTP properties.[96–99] In some cases, the regulation of RTP and TADF properties was realized by forming different crystal systems.[100,101] The investigation on the stimuli-responsive properties of RTP-emissive organic crystals is also important, which often leads to the realization of white light emission.[102,103]

In 2020, Ishi-i and coworkers focused on the polymorph-dependent RTP and multi-stimuli-responsive emission of carbazole–pyrimidine dye **24** (Fig. 9).[104] Two polymorphic crystals **24-A** and **24-B** were obtained from chloroform and chloroform/hexane solution, respectively. The polymorph **24-A** in the space group of *I*2/*a* showed fluorescence–RTP dual emission (λ_{em} = 431 and 546 nm), whereas another polymorph **24-B** showed only a fluorescence band (λ_{em} = 476 nm) in the steady-state fluorescence spectrum. In the crystal structure of **24-A**, twisted molecules were arranged one-dimensionally in an anti-parallel manner. The intermolecular halogen···π interactions were confirmed between the adjacent molecules, which should account for the efficient RTP from the crystalline **24-A**. The emission properties of **24-B** were explained based on the structure of a similar non-phosphorescent crystal **24-B'** in the space group of $P2_1/n$. The molecules in the **24-B'** crystals were more planar than those in the **24-A** crystals. The crystal packing structure of **24-B'** showed the absence of intermolecular halogen interactions, which should rationalize the inactivity of RTP emission. Notably, white-light emission was realized by melting **24-A** followed by cooling to room temperature. Moreover, the ground sample of **24-A** rapidly changed to **24-B** in response to $CHCl_3$ vapor within 0.5 h. The stimuli-responsive switching of **24-A** should be caused by the relatively loose packing of **24-A**.

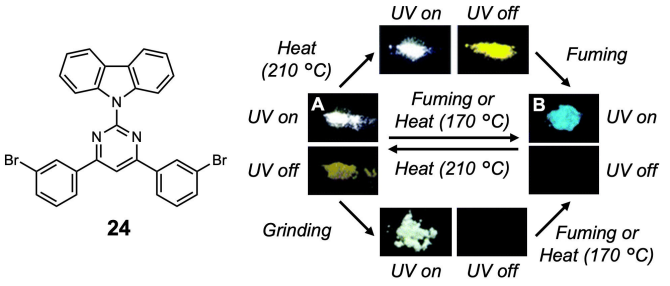

Fig. 9 Polymorph-dependent emission and stimuli-responsive luminescence switching of **24**. Reproduced from Ref. 104 with permission. Copyright 2020 Royal Society of Chemistry.

5. Multi-color-emission by pseudopolymorphs and cocrystals

5.1. Pseudopolymorphic MCL crystals

Pseudopolymorphic (solvent-including) crystals have different molecular arrangements from solvate-free crystals.[14,15] Accordingly, the formation of pseudopolymorphic crystals is a useful strategy to control the emission properties of organic crystals. Moreover, pseudopolymorphs are characterized by their ability to respond readily to a wide variety of external stimuli.[105–107] The luminescent properties of pseudopolymorphs could be changed by the phase transition induced by removing solvent molecules upon heating or by exposing another solvent vapor. The inclusion of solvent molecules often results in the formation of sparse crystal structures with relatively weak intermolecular interactions, leading to high responsiveness toward mechanical stimuli.

In 2019, Li, Tang, and coworkers investigated multistimuli-responsive fluorescence of pseudopolymorphic crystals of TPE derivative **25** bearing two methoxy and one carboxy groups (Fig. 10a).[108] The emission wavelength of weakly blue-emissive crystalline powder of **25** changed from 451 nm to 496 nm upon grinding. The ground **25** was transformed into a weakly blue-emissive state (λ_{em} = 462 nm) or a strongly cyan-emissive state (λ_{em} = 482 nm) after being exposed to acetone or heated to 140 °C, respectively. The weakly blue-emissive crystals, prepared from a CH_2Cl_2 solution, formed porous hydrogen-bonded organic framework (HOF) with the triclinic space group of *P*-1. Pseudopolymorphic HOF crystals containing hexane or acetone in the pores were obtained from CH_2Cl_2/hexane or acetone/H_2O, respectively. These crystals also exhibited weak blue emission. Moreover, another polymorphic crystal ($P2_1/n$) containing CH_2Cl_2 molecules was obtained from CH_2Cl_2/hexane. This monoclinic crystal exhibited intense cyan emission under UV irradiation, which should be attributed to the stronger intermolecular interactions between molecules of **25**. Furthermore, the HOF crystals changed to different crystalline states upon heating to 140 °C that exhibited intense cyan emission. The increase in the emission intensity is rationalized by the destruction of porous HOF structures and the formation of closely stacked arrangements.

In the same year, Zhou, Tian, and coworkers reported the pseudopolymorphic crystals of acridone-substituted TPE derivative **26** (Fig. 10b).[109] The two polymorphs C1 (*P*-1) and C2 ($P2_1/c$) exhibited blue and cyan emission, respectively. The triclinic crystals C1 contained solvent molecules, and therefore the molecular packing of **26** in C1 is looser than that in monoclinic crystals C2. Based on the TD-DFT calculations, the blue and cyan-emission could be assigned as the locally excited (LC) and intramolecular charge-transfer (ICT) state, respectively. The emission color of these polymorphs changed in the bathochromic direction upon grinding, and the ground C1 was transformed into C2 after being heated.

Devi and Sarma examined the MCL of polymorphic crystals of 2-hydroxynaphthaldehyde semicarbazone **27** in 2019 (Fig. 10c).[110] Non-emissive crystals ($P2_1/n$) containing methanol molecules and weakly yellow-emissive crystals ($P2_1/c$) prepared from THF were transformed into bright green-emissive forms upon grinding. The bright green emission should be attributed to the reduction in the aromatic stacking interactions. The formation of stronger hydrogen bonds should increase the intensity of green emission owing to the disruption of non-radiative decay processes.

Pseudopolymorphic crystals of a D-A-type benzothiadiazole derivative **28** were reported by Ito and coworkers in 2019 (Fig. 10d).[111] The monoclinic crystal ($P2_1/c$), consisting only of **28** molecules, exhibited green emission, whereas pseudopolymorphic triclinic crystals (*P*-1) containing benzene or toluene molecules showed orange emission. Upon grinding, the emission color of all crystals changed to yellow. The hypsochromic shifts of the emission from the solvent-containing crystals were achieved by amorphization of crystal structures together with the release of solvent molecules.

Mechanical-stimuli-responsive release of solvent molecules from a pseudopolymorphic crystal was also reported by Sagara and coworkers in 2021 (Fig. 10e).[112] 9,10-Bis(phenylethynyl)anthracene-based cyclophane **29** formed $CHCl_3$-containing crystals **29-YG**, which exhibited the emission-color switching from yellow-green to yellow upon grinding with releasing $CHCl_3$ molecules. Meanwhile, the solvate-free crystal **29-Y** exhibited the hypsochromic shift of the emission from yellow to green upon gentle crushing followed by the bathochromic shift of the emission owing to the formation of excimers in response to grinding stimuli.

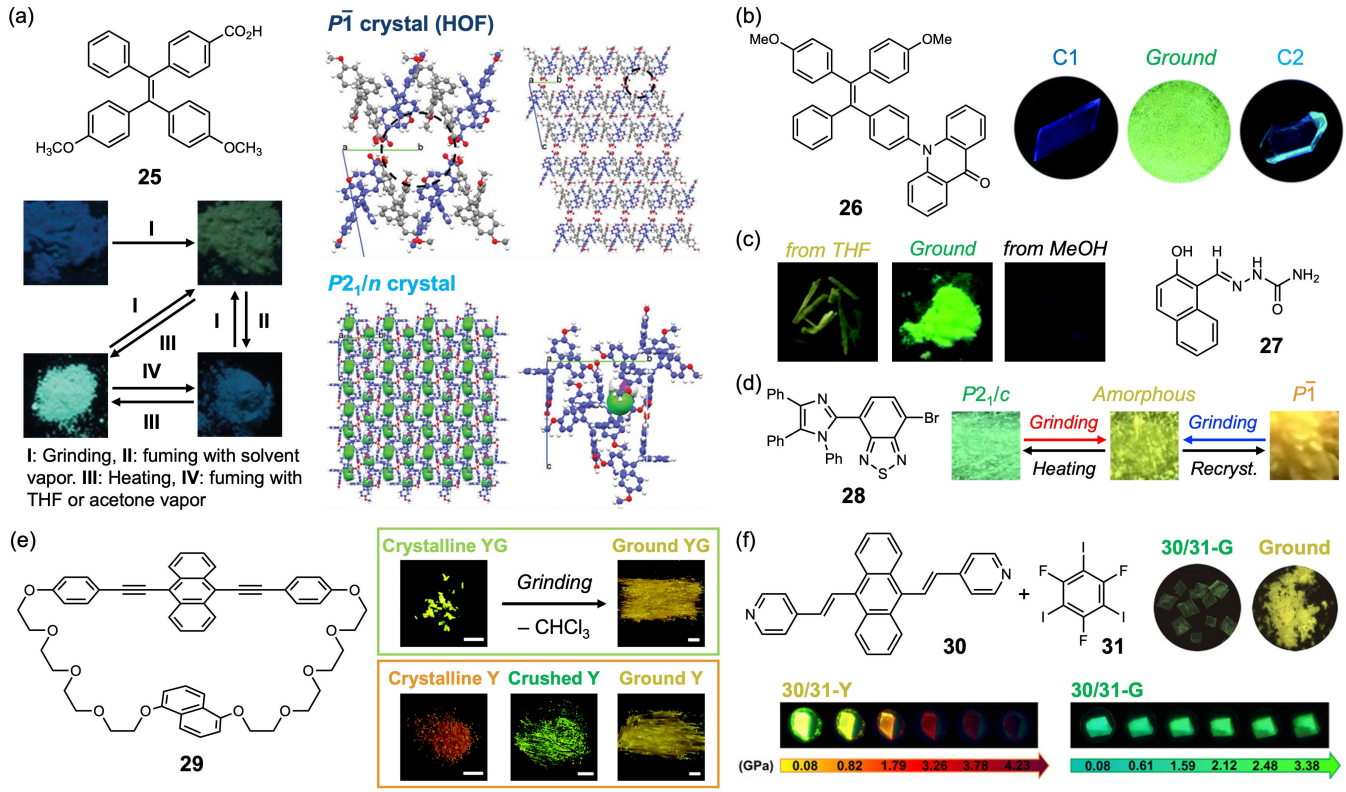

Fig. 10 (a) Photographs of the stimuli-responsive emission switching under UV (left) and crystal structures of pseudopolymorphs (right) of **25**. (b–d) Photographs of pseudopolymorphs and ground samples of **26**–**28** under UV. (e) Photographs of stimuli-responsive switching of pseudopolymorphs of **29** under UV. (f) Photographs of crystalline and ground **30/31-G** under UV (top) and piezochromic luminescence of **30/31-Y** and **30/31-G**. (a and f) Reproduced from Refs. 108 and 117 with permission. Copyright 2019 and 2020 Wiley-VCH Verlag GmbH & Co. KGaA, Weinheim. (b, c, and e) Reproduced from Refs. 109, 110, and 112 with permission. Copyright 2019 and 2021 Royal Society of Chemistry. (d) Reproduced from Ref. 111 with permission. Copyright 2019 The Chemical Society of Japan.

5.2. MCL of polymorphic cocrystals

The formation of cocrystals from a luminescent compound with another luminescent or non-luminescent solid compound is an efficient strategy to tune the emission properties of organic crystals. Nevertheless, only recently, a few examples of mechanical-stimuli-responsive cocrystals have been reported.[113–116] Accordingly, little is known about the differences in luminescent and stimuli-response properties exhibited by polymorphic cocrystals.

A pioneering example of the multi-stimuli-responsive fluorescence switching of polymorphic cocrystals was reported by Xu and coworkers in 2020 (Fig. 10f).[117] Two polymorphic crystals were obtained from 9,10-bis[(*E*)-2-(pyridin-4-yl)vinyl]anthracene (**30**) and 1,3,5-trifluoro-2,4,6-triiodobenzene (**31**). The triclinic polymorph **30/31-Y** (*P*-1) exhibited intense yellow emission, whereas weak green emission was observed from the other monoclinic polymorph **30/31-G** ($P2_1/c$). The yellow-emissive polymorph **30/31-Y** changed to the weakly green-emissive polymorph **30/31-G** in response to THF vapor or heating. Upon grinding, the green-emissive **30/31-G** were converted into yellow-emissive amorphous states. The yellow emission of **30/31-Y** is rationalized by the formation of J-aggregates of **30** molecules, whereas the adjacent molecules of **30** and **31** formed local coplanar H-aggregates in **30/31-G** polymorph. A remarkable red shift of the emission by 92 nm was observed under the hydrostatic compression of **30/31-Y** to 3.26 GPa. In contrast, the red shift of the emission of **30/31-G** under the same hydrostatic pressure was only 24 nm. The larger shift in the emission wavelength of **30/31-Y** should be attributed to the increased exciton coupling between neighboring **30** chromophores.

6. Other mechanical properties of polymorphic crystals

6.1. Mechanoluminescence (ML) polymorphic crystals

Mechanoluminescence (ML), also known as triboluminescence, is a phenomenon in which excited molecules generated by mechanical stimuli exhibit luminescence without the irradiation of excitation light.[118,119] Regardless of the recent intensive investigations on the ML-active organic crystals,[78,120–124] the underlying physical process of ML has not yet been fully elucidated. A promising mechanism of the TL process is the electronic excitation of luminescent molecules induced by fracturing the surface of organic crystals. Since molecular packing structures should have a significant impact on the ML properties, several polymorphic crystals have recently been investigated to understand the relationship between crystal structures and ML properties.[36,125–128]

Very recent studies have focused on the polymorphic crystals exhibiting different phosphorescence and ML properties depending on the packing structures of luminescent molecules. In 2019, Q. Li, Z. Li, and coworkers revealed the preferential packing modes for ML and RTP of TPA derivative **32** that formed two polymorphic crystals (Fig. 11a).[129] Block-like crystals of **32** (crystal A: *P*-1) showed yellow RTP without ML property, whereas lamellar crystals of **32** (crystal B: *Pn*) exhibited ML without RTP property. In each unit cell of crystal A, two molecules with slightly different conformations were observed. These molecules formed a tight molecular packing with an anti-parallel arrangement, which would contribute to the RTP effect. Moreover, TD-DFT calculation suggested that the intersystem crossing (ISC) process to afford RTP should be facilitated for the dimer structure of **32** in the crystal A. In contrast, the unit cell of crystal B contained six molecules with different conformations. The solid-state ^{13}C NMR analysis revealed that the ML-active crystal B formed inhomogeneous layered structures with different strengths of intermolecular interactions. Accordingly, the charge accumulation required to generate the excited states of **32** molecules should be caused by the mechanical-stimuli-induced destruction of crystal structures at the weakly interacting layers. The polymorphic crystals of carbazole-derivative **33** that exhibit both RTP and ML were reported by Huang, Li, Tang, and coworkers in 2021 (Fig. 11b).[130] Colorful ML was also achieved by mixing **33**, showing near-ultraviolet ML, with other luminescent dyes. In the same year, C. Xu, Zhao, B. Xu, and coworkers also reported the dual-mode persistent luminescence and ML for the two polymorphs of carbazole derivative **34** (Fig. 11c).[131] The orthorhombic ($P2_12_12_1$) crystals of **34** exhibited afterglows composed of persistent TADF and ultralong organic phosphorescence owing to the strong intermolecular interactions in the crystals. In contrast, monoclinic ($P2_1$) crystals of **34** were ML-active, which should be attributed to the formation of polar space groups with helical molecular arrangements.

6.2. Mechanical deformation of polymorphic crystals

Flexible organic crystals that can change their shape responding to external mechanical stimuli have attracted recent interest because of their potential to provide wide applications.[132–134] The mechanoresponsive behaviors of organic crystals are typically classified into reversible elastic bending and irreversible plastic deformation. Although the deformability of organic crystals should be determined by molecular packing structures, luminescent polymorphic crystals with distinctly different flexibility have scarcely been obtained. In 2020, Zhang and coworkers reported the rare example of polymorphic crystals that exhibit remarkable mechanical behaviors (Fig. 11d).[135] Diaryl β-diketone **35** was crystallized in green-, yellow-, and orange-emissive polymorphs **35-G** (*Pbca*), **35-Y** ($P2_1/c$), and **35-O** ($P2_1/c$), which exhibited elastic, plastic, and brittle property, respectively. Owing to the large overlap between π-stacked molecules, molecules in **35-O** should form the strongest π-stacking interactions. Meanwhile, **35-G** exhibited only a slight π-stacking interaction. Such difference should account for the red-shifted emission from **35-O**. In addition, the brittle nature of **35-O** was explained by the absence of sliding planes in the condensed packing structure. In contrast, isotropic intermolecular interactions and a crosswise packing structure were observed for **35-G**, which should contribute to the elastic property of the crystal. In the case of the plastic polymorph **35-Y**, molecules were arranged in a layered structure, which

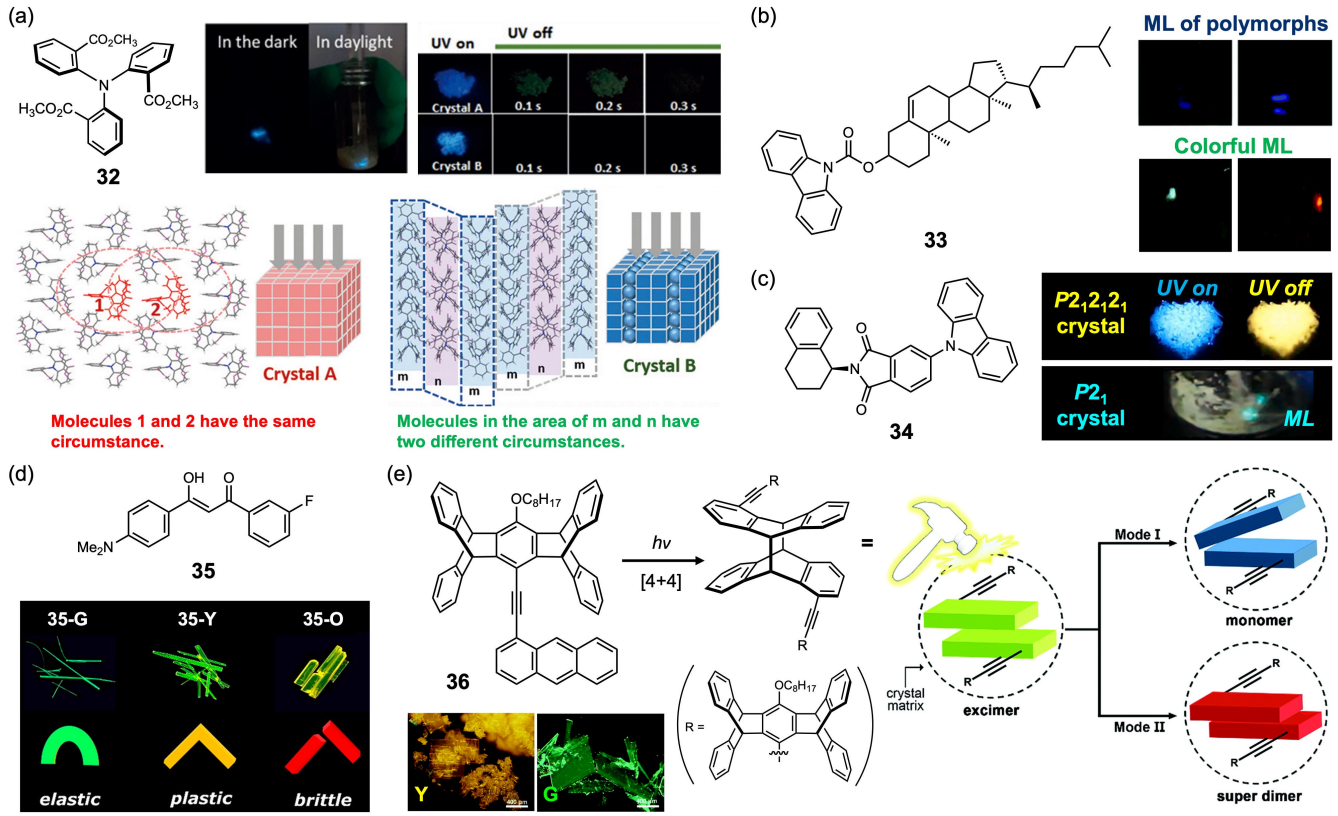

Fig. 11 (a) Photographs of the ML and RTP of **32** (top) and crystal structures of polymorphs of **32** (bottom). Reproduced from Ref. 129 with permission. Copyright 2019 Wiley-VCH Verlag GmbH & Co. KGaA, Weinheim. (b) Photographs of ML of **33** and **33** with other luminescent dyes. Reproduced from Ref. 130 with permission. Copyright 2021 Royal Society of Chemistry. (c) Photographs of RTP and ML of **34**. Reproduced from Ref. 131 with permission. Copyright 2021 Elsevier. (d) Mechanical deformations of polymorphs of **35**. Reproduced from Ref. 135 with permission. Copyright 2020 American Chemical Society. (e) Proposed mechanisms for the PMFC of **36**. Reproduced from Ref. 136 with permission. Copyright 2018 Royal Society of Chemistry.

provided efficient space for the molecular sliding induced by external mechanical force.

6.3. Photomechanofluorochromism (PMFC) of polymorphic crystals

Not limited to external mechanical forces, internal photomechanical forces can switch the luminescent properties of organic crystals by altering intermolecular interactions. A rare example of photomechanofluorochromism (PMFC) was developed by Yang and coworkers in 2018 (Fig. 11e).[136] Pentiptycene derivative **36** formed yellow-emissive and green-emissive polymorphs **36-Y** and **36-G** in the same space group $P2_1/c$ with different molecular arrangements. Upon irradiation with UV light, the photodimerization of the stacked anthracene groups of **36** occurred for both polymorphs, and the resulting dimer exerted photomechanical stresses on the adjacent molecules in the crystals. In response to photomechanical stresses, the yellow emission of **36-Y** changed to blue via white emission owing to the alteration from excimer to monomer emission of **36**. The original **36-Y** was recovered by heating the photomechanically changed state. On the other hand, the emission color of **36-G** was shifted in the bathochromic direction to red by photomechanical stresses. The formation of super dimers should account for the red-shifted emission of the photomechanically generated state from **36-G**. When the resulting red-emissive state was irradiated with visible light of 580 nm, the fluorescence color recovered to yellowish green.

7. Summary and perspective

This highlight has summarized recent progress on the luminescent polymorphic crystals exhibiting versatile mechanoresponsive properties. Section 2 has described the recent advances in fluorescent MCL crystals. The formation of polymorphic crystals has been shown as an effective method to tune the emission color of a single fluorescent compound. Typically, the degree of MCL shift depends on the initial fluorescence color of polymorphic crystals, and the ground amorphous samples of polymorphic crystals often exhibit a similar emission color. As shown in Section 3, the stimuli-responsive property of organic crystals could be altered by forming different packing structures. The formation of polymorphic crystals can control the amount of wavelength change in two-step MCL. In addition, two-step MCL including

phase transition between polymorphs has been realized. The introduction of acid-responsive moieties has shown as a reliable method to achieve multi-stimuli-responsive emission by polymorphic crystals. Section 4 has highlighted the tuning of TADF and RTP properties of organic crystals based on the structural alterations of polymorphs. As exemplified by the realization of white light emission, research on organic crystals that realize the control of dual emission by external stimuli is expected to attract more attention in the near future. Recent achievements regarding the tuning of MCL properties by forming pseudopolymorphs and cocrystals have been summarized in Section 5. Pseudopolymorphic crystals of HOF and macrocyclic compounds have emerged, and the host–guest chemistry in crystalline MCL compounds will become an important research field in obtaining organic crystals with controlled luminescence properties. In Section 6, mechanoresponsive polymorphs other than MCL crystals have been briefly introduced. Based on the analysis of polymorphic crystals, the structural features required for ML-active crystals have been gradually revealed.

The majority of fluorophores summarized in this highlight are donor-acceptor (D-A)-type compounds that can exhibit intramolecular charge-transfer (ICT) emission. Since the ICT emission is sensitive to molecular conformation and intermolecular interactions, the emission color of D-A-type fluorophores is variable to the alteration of molecular arrangements caused by forming polymorphs or amorphization. Some TADF polymorphs have shown multicolor emission solely due to differences in intermolecular interactions of the emitters, even when there are little changes in molecular conformations.[88,90,92] It is rare to switch the emission color between the locally excited emission and the ICT emission.[109] In the case of other fluorophores that do not exhibit ICT, the formation of J- or H-aggregates is a typical main reason for the remarkable shifts in emission wavelength depending on the molecular arrangement.[56,74] In a limited number of cases, the mechanoresponsive shift of emission wavelength has originated from the switching between monomer and excimer emission.[112] Increased exciton coupling has also been proposed to explain the emission switching induced by hydrostatic compression.[117]

As highlighted in this article, it has become possible to obtain organic fluorescent crystals that exhibit a variety of MCL properties other than the typical bicolor MCL. In addition to the fluorescent compounds, significant progress has also been made in the development of polymorphic crystals showing triplet-related TADF and RTP. Another attractive luminescence is circularly polarized luminescence (CPL) by chiral luminophores. In contrast to the recent intensive studies on the CPL-emissive organic small molecules in solution states,[137–139] the MCL behavior of CPL-emissive organic crystals is still less explored.[140–142] Further investigations on the mechanoresponsive properties of chiral polymorphic crystals will be necessary. From the viewpoint of the computational prediction of crystal structures, highly accurate methods have been developed owing to the recent improvements in computer performance.[143] However, it is still difficult to predict the effect of the crystal structure on luminescence and stimuli-responsive properties.[144,145] By accumulating experimental findings from extensive studies of polymorphic crystals, the accuracy of the computational prediction is expected to increase in the future. Establishing reliable methods to predict and control the structure and luminescent properties of organic crystals are highly desirable for the deep understanding of fundamental chemistry and the development of practical materials with advanced luminescent properties.

Conflicts of interest

The author declares no conflicts of interest.

Acknowledgements

This work was partly supported by JSPS KAKENHI Grant Number JP20K05645 within the Grant-in-Aid for Scientific Research (C), JSPS KAKENHI Grant Number JP20H04665 within the Grant-in-Aid for Scientific Research on Innovative Areas “Soft Crystals: Area No. 2903”, and JST, PRESTO Grant Number JPMJPR21A3, Japan.

References

1 J. Gierschner, J. Shi, B. Milián-Medina, D. Roca-Sanjuán, S. Varghese and S. Y. Park, *Adv. Opt. Mater.*, 2021, **9**, 2002251.
2 M. K. Bera, P. Pal and S. Malik, *J. Mater. Chem. C*, 2020, **8**, 788–802.
3 J. Mei, Y. Hong, J. W. Y. Lam, A. Qin, Y. Tang and B. Z. Tang, *Adv. Mater.*, 2014, **26**, 5429–5479.
4 M. Shimizu and T. Hiyama, *Chem. - Asian J.*, 2010, **5**, 1516–1531.
5 Z. Yang, Z. Mao, Z. Xie, Y. Zhang, S. Liu, J. Zhao, J. Xu, Z. Chi and M. P. Aldred, *Chem. Soc. Rev.*, 2017, **46**, 915–1016.
6 Y. Tao, K. Yuan, T. Chen, P. Xu, H. Li, R. Chen, C. Zheng, L. Zhang and W. Huang, *Adv. Mater.*, 2014, **26**, 7931–7958.
7 H. Uoyama, K. Goushi, K. Shizu, H. Nomura and C. Adachi, *Nature*, 2012, **492**, 234–238.
8 W. Jia, Q. Wang, H. Shi, Z. An and W. Huang, *Chem. - Eur. J.*, 2020, **26**, 4437–4448.
9 C.-R. Wang, Y.-Y. Gong, W.-Z. Yuan and Y.-M. Zhang, *Chin. Chem. Lett.*, 2016, **27**, 1184–1192.
10 O. Bolton, K. Lee, H.-J. Kim, K. Y. Lin and J. Kim, *Nat. Chem.*, 2011, **3**, 205–210.
11 M. R. Caira, *Top. Curr. Chem.*, 1998, **198**, 163–208.
12 A. J. Cruz-Cabeza and J. Bernstein, *Chem. Rev.*, 2014, **114**, 2170–2191.
13 D. Gentili, M. Gazzano, M. Melucci, D. Jones and M. Cavallini, *Chem. Soc. Rev.*, 2019, **48**, 2502–2517.
14 D. Giron, *J. Therm. Anal. Calorim.*, 2001, **64**, 37–60.
15 A. Nangia, *Cryst. Growth Des.*, 2006, **6**, 2–4.
16 D. Singhal and W. Curatolo, *Adv. Drug Delivery Rev.*, 2004, **56**, 335–347.
17 N. Chieng, T. Rades and J. Aaltonen, *J. Pharm. Biomed. Anal.*, 2011, **55**, 618–644.
18 D. Yan and D. G. Evans, *Mater. Horiz.*, 2014, **1**, 46–57.
19 S. P. Anthony, *ChemPlusChem*, 2012, **77**, 518–531.
20 Z. Ma, Z. Wang, M. Teng, Z. Xu and X. Jia, *ChemPhysChem*, 2015, **16**, 1811–1828.
21 M. Kato, H. Ito, M. Hasegawa and K. Ishii, *Chem. - Eur. J.*, 2019, **25**, 5105–5112.

22 T. Seki and H. Ito, *Chem. - Eur. J.*, 2016, **22**, 4322–4329.
23 Y. Sagara, S. Yamane, M. Mitani, C. Weder and T. Kato, *Adv. Mater.*, 2016, **28**, 1073–1095.
24 X. Huang, L. Qian, Y. Zhou, M. Liu, Y. Cheng and H. Wu, *J. Mater. Chem. C*, 2018, 6, 5075–5096.
25 S. Ito, *Chem. Lett.*, 2021, *50*, 649–660.
26 T. Mutai, H. Tomoda, T. Ohkawa, Y. Yabe and K. Araki, *Angew. Chem., Int. Ed.*, 2008, **47**, 9522–9524.
27 N. S. S. Kumar, S. Varghese, N. P. Rath and S. Das, *J. Phys. Chem. C*, 2008, **112**, 8429–8437.
28 P. Galer, R. C. Korošec, M. Vidmar and B. Šket, *J. Am. Chem. Soc.*, 2014, **136**, 7383–7394.
29 Z. Lin, X. Mei, E. Yang, X. Li, H. Yao, G. Wen, C.-T. Chien, T. J. Chow and Q. Ling, *CrystEngComm*, 2014, **16**, 11018–11026.
30 Z. He, L. Zhang, J. Mei, T. Zhang, J. W. Y. Lam, Z. Shuai, Y. Q. Dong and B. Z. Tang, *Chem. Mater.*, 2015, **27**, 6601–6607.
31 M. Li, Q. Zhang, J.-R. Wang and X. Mei, *Chem. Commun.*, 2016, **52**, 11288–11291.
32 S. Varughese, *J. Mater. Chem. C*, 2014, **2**, 3499–3516.
33 B. Lu, S. Liu and D. Yan, *Chin. Chem. Lett.*, 2019, **30**, 1908–1922.
34 Z. Zhao, J. W. Y. Lam and B. Z. Tang, *J. Mater. Chem.*, 2012, **22**, 23726–23740.
35 J. Tong, Y. Wang, J. Mei, J. Wang, A. Qin, J. Z. Sun and B. Z. Tang, *Chem. - Eur. J.*, 2014, **20**, 4661–4670.
36 B. Xu, J. He, Y. Mu, Q. Zhu, S. Wu, Y. Wang, Y. Zhang, C. Jin, C. Lo, Z. Chi, A. Lien, S. Liu and J. Xu, *Chem. Sci.*, 2015, **6**, 3236–3241.
37 Y. Lin, G. Chen, L. Zhao, W. Z. Yuan, Y. Zhang and B. Z. Tang, *J. Mater. Chem. C*, 2015, **3**, 112–120.
38 M. Salimimarand, D. D. La, M. Al Kobaisi and S. V. Bhosale, *Sci. Rep.*, 2017, **7**, 42898.
39 J.-Y. Zhu, C.-X. Li, P.-Z. Chen, Z. Ma, B. Zou, L.-Y. Niu, G. Cui and Q.-Z. Yang, *Mater. Chem. Front.*, 2020, **4**, 176–181.
40 X. Wang, C. Qi, Z. Fu, H. Zhang, J. Wang, H.-T. Feng, K. Wang, B. Zou, J. W. Y. Lam and B. Z. Tang, *Mater. Horiz.*, 2021, **8**, 630–638.
41 P. S. Hariharan, D. Moon and S. P. Anthony, *J. Mater. Chem. C*, 2015, **3**, 8381–8388.
42 P. S. Hariharan, N. S. Venkataramanan, D. Moon and S. P. Anthony, *J. Phys. Chem. C*, 2015, **119**, 9460–9469.
43 P. S. Hariharan, V. K. Prasad, S. Nandi, A. Anoop, D. Moon and S. P. Anthony, *Cryst. Growth Des.*, 2017, **17**, 146–155.
44 P. S. Hariharan, G. Parthasarathy, A. Kundu, S. Karthikeyan, Y. Sagara, D. Moon and S. P. Anthony, *Cryst. Growth Des.*, 2018, **18**, 3971–3979.
45 C. Zhu, Q. Luo, Y. Shen, C. Lv, S. Zhao, X. Lv, F. Cao, K. Wang, Q. Song, C. Zhang and Y. Zhang, *Angew. Chem., Int. Ed.*, 2021, **60**, 8510–8514.
46 T. Ishi-i, H. Tanaka, R. Kichise, C. Davin, T. Matsuda, N. Aizawa, I. S. Park, T. Yasuda and T. Matsumoto, *Chem. - Asian J.*, 2021, **16**, 2136–2145.
47 S. Ito, T. Yamada, T. Taguchi, Y. Yamaguchi and M. Asami, *Chem. - Asian J.*, 2016, **11**, 1963–1970.
48 S. Ito, T. Taguchi, T. Yamada, T. Ubukata, Y. Yamaguchi and M. Asami, *RSC Adv.*, 2017, **7**, 16953–16962.
49 S. Nagai, M. Yamashita, T. Tachikawa, T. Ubukata, M. Asami and S. Ito, *J. Mater. Chem. C*, 2019, **7**, 4988–4998.
50 M. Yamashita, S. Nagai, S. Ito and T. Tachikawa, *J. Phys. Chem. Lett.*, 2021, **12**, 7826–7831.
51 S. Ito, S. Nagai, T. Ubukata, T. Ueno and H. Uekusa, *Cryst. Growth Des.*, 2020, **20**, 4443–4453.
52 S. Ito, S. Nagai, T. Ubukata and T. Tachikawa, *CrystEngComm*, 2021, **23**, 5899–5907.
53 J. W. Chung, Y. You, H. S. Huh, B.-K. An, S.-J. Yoon, S. H. Kim, S. W. Lee and S. Y. Park, *J. Am. Chem. Soc.*, 2009, **131**, 8163–8172.
54 M. Martínez-Abadía, R. Giménez and M. B. Ros, *Adv. Mater.*, 2018, **30**, 1704161.
55 W. Yang, C. Liu, S. Lu, J. Du, Q. Gao, R. Zhang, Y. Liu and C. Yang, *J. Mater. Chem. C*, 2018, **6**, 290–298.
56 H.-J. Kim, J. Gierschner and S. Y. Park, *J. Mater. Chem. C*, 2020, **8**, 7417–7421.
57 J. Guan, F. Xu, C. Tian, L. Pu, M.-S. Yuan and J. Wang, *Chem. - Asian J.*, 2019, **14**, 216–222.
58 G. Chen, W.-C. Chen, S. Ji, P. Zhou, N. Cai, Y. Zhan, H. Liang, J.-H. Tan, C. Pan and Y. Huo, *CrystEngComm*, 2020, **22**, 2147–2157.
59 Z. Wang, M. Wang, J. Peng, Y. Xie, M. Liu, W. Gao, Y. Zhou, X. Huang and H. Wu, *J. Phys. Chem. C*, 2019, **123**, 27742–27751.
60 Z. Ma, M. Teng, Z. Wang, S. Yang and X. Jia, *Angew. Chem., Int. Ed.*, 2013, **52**, 12268–12272.
61 S. Ito, T. Yamada and M. Asami, *ChemPlusChem*, 2016, **81**, 1272–1275.
62 Z. Ma, Z. Wang, X. Meng, Z. Ma, Z. Xu, Y. Ma and X. Jia, *Angew. Chem., Int. Ed.*, 2016, **55**, 519–522.
63 X. Wu, J. Guo, Y. Cao, J. Zhao, W. Jia, Y. Chen and D. Jia, *Chem. Sci.*, 2018, **9**, 5270–5277.
64 S. Ito, R. Sekine, M. Munakata, M. Yamashita and T. Tachikawa, *Chem. - Eur. J.*, 2021, **27**, 13982–13990.
65 Y. Dong, B. Xu, J. Zhang, X. Tan, L. Wang, J. Chen, H. Lv, S. Wen, B. Li, L. Ye, B. Zou and W. Tian, *Angew. Chem., Int. Ed.*, 2012, **51**, 10782–10785.
66 Y. Wang, W. Liu, L. Ren and G. Ge, *Mater. Chem. Front.*, 2019, **3**, 1661–1670.
67 S. Saotome, K. Suenaga, K. Tanaka and Y. Chujo, *Mater. Chem. Front.*, 2020, **4**, 1781–1788.
68 S. Takahashi, S. Nagai, M. Asami and S. Ito, *Mater. Adv.*, 2020, **1**, 708–719.
69 X.-L. Lu and M. Xia, *J. Mater. Chem. C*, 2016, **4**, 9350–9358.
70 F. Wang, C. A. DeRosa, M. L. Daly, D. Song, M. Sabat and C. L. Fraser, *Mater. Chem. Front.*, 2017, **1**, 1866–1874.
71 B. Roy, M. C. Reddy and P. Hazra, *Chem. Sci.*, 2018, **9**, 3592–3606.
72 S. Ito, C. Nishimoto and S. Nagai, *CrystEngComm*, 2019, **21**, 5699–5706.
73 W. Yang, Y. Yang, Y. Qiu, X. Cao, Z. Huang, S. Gong and C. Yang, *Mater. Chem. Front.*, 2020, **4**, 2047–2053.
74 B. Shao, R. Jin, A. Li, Y. Liu, B. Li, S. Xu, W. Xu, B. Xu and W. Tian, *J. Mater. Chem. C*, 2019, **7**, 3263–3268.
75 Y.-X. Li, Y.-G. Chen, Z.-F. Yu, X.-F. Yang, Y. Nie, Y. Cui and G.-X. Sun, *J. Phys. Chem. C*, 2020, **124**, 3784–3792.
76 P. Gayathri, M. Pannipara, A. G. Al-Sehemi, D. Moon and S. P. Anthony, *Mater. Adv.*, 2021, **2**, 996–1005.
77 D. T. Hogan, B. S. Gelfand, D. M. Spasyuk and T. C. Sutherland, *Mater. Chem. Front.*, 2020, **4**, 268–276.
78 S. Xu, T. Liu, Y. Mu, Y.-F. Wang, Z. Chi, C.-C. Lo, S. Liu, Y. Zhang, A. Lien and J. Xu, *Angew. Chem., Int. Ed.*, 2015, **54**, 874–878.
79 Y. Zhang, H. Ma, S. Wang, Z. Li, K. Ye, J. Zhang, Y. Liu, Q. Peng and Y. Wang, *J. Phys. Chem. C*, 2016, **120**, 19759–19767.
80 Y. Zhang, Y. Miao, X. Song, Y. Gao, Z. Zhang, K. Ye and Y. Wang, *J. Phys. Chem. Lett.*, 2017, **8**, 4808–4813.
81 I. Hladka, D. Volyniuk, O. Bezvikonnyi, V. Kinzhybalo, T. J. Bednarchuk, Y. Danyliv, R. Lytvyn, A. Lazauskas and J. V. Grazulevicius, *J. Mater. Chem. C*, 2018, **6**, 13179–13189.
82 X. Cai, Z. Qiao, M. Li, X. Wu, Y. He, X. Jiang, Y. Cao and S.-J. Su, *Angew. Chem., Int. Ed.*, 2019, **58**, 13522–13531.
83 B. Xu, Y. Mu, Z. Mao, Z. Xie, H. Wu, Y. Zhang, C. Jin, Z. Chi, S. Liu, J. Xu, Y.-C. Wu, P.-Y. Lu, A. Lien and M. R. Bryce, *Chem. Sci.*, 2016, **7**, 2201–2206.
84 M. Okazaki, Y. Takeda, P. Data, P. Pander, H. Higginbotham, A. P. Monkman and S. Minakata, *Chem. Sci.*, 2017, **8**, 2677–2686.
85 B. Huang, Z. Li, H. Yang, D. Hu, W. Wu, Y. Feng, Y. Sun, B. Lin and W. Jiang, *J. Mater. Chem. C*, 2017, **5**, 12031–12034.
86 R. Pashazadeh, P. Pander, A. Lazauskas, F. B. Dias and J. V. Grazulevicius, *J. Phys. Chem. Lett.*, 2018, **9**, 1172–1177.
87 P. Data and Y. Takeda, *Chem. - Asian J.*, 2019, **14**, 1613–1636.

88 B. Huang, W.-C. Chen, Z. Li, J. Zhang, W. Zhao, Y. Feng, B. Z. Tang and C. S.-Lee, *Angew. Chem., Int. Ed.*, 2018, **57**, 12473–12477.
89 K. Zheng, F. Ni, Z. Chen, C. Zhong and C. Yang, *Angew. Chem., Int. Ed.*, 2020, **59**, 9972–9976.
90 W. Yang, Y. Yang, L. Zhan, K. Zheng, Z. Chen, X. Zeng, S. Gong and C. Yang, *Chem. Eng. J.*, 2020, **390**, 124626.
91 W. Yang, Y. Yang, X. Cao, Y. Liu, Z. Chen, Z. Huang, S. Gong and C. Yang, *Chem. Eng. J.*, 2021, **415**, 128909.
92 H. Yu, X. Song, N. Xie, J. Wang, C. Li and Y. Wang, *Adv. Funct. Mater.*, 2021, **31**, 2007511.
93 A. Forni, E. Lucenti, C. Botta and E. Cariati, *J. Mater. Chem. C*, 2018, **6**, 4603–4626.
94 L. Xiao and H. Fu, *Chem. - Eur. J.*, 2019, **25**, 714–723.
95 T. Zhang, X. Ma, H. Wu, L. Zhu, Y. Zhao and H. Tian, *Angew. Chem., Int. Ed.*, 2020, **59**, 11206–11216.
96 T. Zhang, Z. Zhao, H. Ma, Y. Zhang and W. Z. Yuan, *Chem. - Asian J.*, 2019, **14**, 884–889.
97 E. Lucenti, A. Forni, A. Previtali, D. Marinotto, D. Malpicci, S. Righetto, C. Giannini, T. Virgili, P. Kabacinski, L. Ganzer, U. Giovanella, C. Botta and E. Cariati, *Chem. Sci.*, 2020, **11**, 7599–7608.
98 W. Che, Y. Gong, L. Tu, M. Han, X. Li, Y. Xie and Z. Li, *Phys. Chem. Chem. Phys.*, 2020, **22**, 21445–21452.
99 H. Liu, W. Liu, N. Ando, S. Yamaguchi and H. Zhang, *J. Mater. Chem. C*, 2021, **9**, 2738–2743.
100 C. Chen, R. Huang, A. S. Batsanov, P. Pander, Y.-T. Hsu, Z. Chi, F. B. Dias and M. R. Bryce, *Angew. Chem., Int. Ed.*, 2018, **57**, 16407–16411.
101 S. Li, L. Fu, X. Xiao, H. Geng, Q. Liao, Y. Liao and H. Fu, *Angew. Chem., Int. Ed.*, 2021, **60**, 18059–18064.
102 B. Xu, H. Wu, J. Chen, Z. Yang, Z. Yang, Y.-C. Wu, Y. Zhang, C. Jin, P.-Y. Lu, Z. Chi, S. Liu, J. Xu and M. Aldred, *Chem. Sci.*, 2017, **8**, 1909–1914.
103 Y. Liu, Z. Ma, J. Liu, M. Chen, Z. Ma and X. Jia, *Adv. Opt. Mater.*, 2021, **9**, 2001685.
104 T. Ishi-i, H. Tanaka, I. S. Park, T. Yasuda, S. Kato, M. Ito, H. Hiyoshi and T. Matsumoto, *Chem. Commun.*, 2020, **56**, 4051–4054.
105 Y. Chen, Z. Peng, Y. Tao, Z. Wang, P. Lu and Y. Wang, *Dyes Pigm.*, 2019, **161**, 44–50.
106 J. Fang, Q. Zhang, M. Li, J.-R. Wang and X. Mei, *ACS Omega*, 2018, **3**, 9220–9226.
107 P.-Z. Chen, H. Zhang, L.-Y. Niu, Y. Zhang, Y.-Z. Chen, H.-B. Fu and Q.-Z. Yang, *Adv. Funct. Mater.*, 2017, **27**, 1700332.
108 G. Huang, Y. Jiang, S. Yang, B. S. Li and B. Z. Tang, *Adv. Funct. Mater.*, 2019, **29**, 1900516.
109 S. Jiang, J. Wang, Q. Qi, J. Qian, B. Xu, F. Li, Q. Zhou and W. Tian, *Chem. Commun.*, 2019, **55**, 3749–3752.
110 K. Devi and R. J. Sarma, *CrystEngComm*, 2019, **21**, 4811–4819.
111 S. Ito, S. Nagai, T. Ubukata and M. Asami, *Chem. Lett.*, 2019, **48**, 1492–1495.
112 Y. Sagara, K. Takahashi, A. Seki, T. Muramatsu, T. Nakamura and N. Tamaoki, *J. Mater. Chem. C*, 2021, **9**, 1671–1677.
113 G. Fan and D. Yan, *Sci. Rep.*, 2014, **4**, 4933.
114 S. K. Park, I. Cho, J. Gierschner, J. H. Kim, J. H. Kim, J. E. Kwon, O. K. Kwon, D. R. Whang, J.-H. Park, B.-K. An and S. Y. Park, *Angew. Chem., Int. Ed.*, 2016, **55**, 203–207.
115 Y. Liu, Q. Zeng, B. Zou, Y. Liu, B. Xu and W. Tian, *Angew. Chem., Int. Ed.*, 2018, **57**, 15670–15674.
116 Z. Wang, F. Yu, W. Chen, J. Wang, J. Liu, C. Yao, J. Zhao, H. Dong, W. Hu and Q. Zhang, *Angew. Chem., Int. Ed.*, 2020, **59**, 17580–17586.
117 Y. Liu, A. Li, S. Xu, W. Xu, Y. Liu, W. Tian and B. Xu, *Angew. Chem., Int. Ed.*, 2020, **59**, 15098–15103.
118 Y. Xie and Z. Li, *Chem*, 2018, **4**, 943–971.
119 S. Mukherjee and P. Thilagar, *Angew. Chem., Int. Ed.*, 2019, **58**, 7922–7932.
120 B. Xu, W. Li, J. He, S. Wu, Q. Zhu, Z. Yang, Y.-C. Wu, Y. Zhang, C. Jin, P.-Y. Lu, Z. Chi, S. Liu, J. Xu and M. R. Bryce, *Chem. Sci.*, 2016, **7**, 5307–5312.
121 J. Yang, Z. Ren, Z. Xie, Y. Liu, C. Wang, Y. Xie, Q. Peng, B. Xu, W. Tian, F. Zhang, Z. Chi, Q. Li and Z. Li, *Angew. Chem., Int. Ed.*, 2017, **56**, 880–884.
122 J. Yang, X. Gao, Z. Xie, Y. Gong, M. Fang, Q. Peng, Z. Chi and Z. Li, *Angew. Chem., Int. Ed.*, 2017, **56**, 15299–15303.
123 J.-A. Li, J. Zhou, Z. Mao, Z. Xie, Z. Yang, B. Xu, C. Liu, X. Chen, D. Ren, H. Pan, G. Shi, Y. Zhang and Z. Chi, *Angew. Chem., Int. Ed.*, 2018, **57**, 6449–6453.
124 J. Yang, J. Qin, P. Geng, J. Wang, M. Fang and Z. Li, *Angew. Chem., Int. Ed.*, 2018, **57**, 14174–14178.
125 C. Wang, B. Xu, M. Li, Z. Chi, Y. Xie, Q. Li and Z. Li, *Mater. Horiz.*, 2016, **3**, 220–225.
126 Z. Xie, T. Yu, J. Chen, E. Ubba, L. Wang, Z. Mao, T. Su, Y. Zhang, M. P. Aldred and Z. Chi, *Chem. Sci.*, 2018, **9**, 5787–5794.
127 Y. Yu, Y. Fan, C. Wang, Y. Wei, Q. Liao, Q. Li and Z. Li, *J. Mater. Chem. C*, 2019, **7**, 13759–13763.
128 C. Wang, Y. Yu, Z. Chai, F. He, C. Wu, Y. Gong, M. Han, Q. Li and Z. Li, *Mater. Chem. Front.*, 2019, **3**, 32–38.
129 J. Wang, Z. Chai, J. Wang, C. Wang, M. Han, Q. Liao, A. Huang, P. Lin, C. Li, Q. Li and Z. Li, *Angew. Chem., Int. Ed.*, 2019, **58**, 17297–17302.
130 H. Zhang, H. Ma, W. Huang, W. Gong, Z. He, G. Huang, B. S. Li and B. Z. Tang, *Mater. Horiz.*, 2021, **8**, 2816–2822.
131 J.-A. Li, Z. Song, Y. Chen, C. Xu, S. Li, Q. Peng, G. Shi, C. Liu, S. Luo, F. Sun, Z. Zhao, Z. Chi, Y. Zhang and B. Xu, *Chem. Eng. J.*, 2021, **418**, 129167.
132 E. Ahmed, D. P. Karothu and P. Naumov, *Angew. Chem., Int. Ed.*, 2018, **57**, 8837–8846.
133 S. Das, A. Mondal and C. M. Reddy, *Chem. Soc. Rev.*, 2020, **49**, 8878–8896.
134 T. Seki, N. Hoshino, Y. Suzuki and S. Hayashi, *CrystEngComm*, 2021, **23**, 5686–5696.
135 X. Chu, Z. Lu, B. Tang, B. Liu, K. Ye and H. Zhang, *J. Phys. Chem. Lett.*, 2020, **11**, 5433–5438.
136 L.-Y. Hsu, S. Maity, Y. Matsunaga, Y.-F. Hsu, Y.-H. Liu, S.-M. Peng, T. Shinmyozu and J.-S. Yang, *Chem. Sci.*, 2018, **9**, 8990–9001.
137 J.-L. Ma, Q. Peng and C.-H. Zhao, *Chem. - Eur. J.*, 2019, **25**, 15441–15454.
138 Y. Ohishi and M. Inouye, *Tetrahedron Lett.*, 2019, **60**, 151232.
139 Y. Imai, *Chem. Lett.*, 2021, **50**, 1131–1141.
140 H. Li, H. Li, W. Wang, Y. Tao, S. Wang, Q. Yang, Y. Jiang, C. Zheng, W. Huang and R. Chen, *Angew. Chem., Int. Ed.*, 2020, **59**, 4756–4762.
141 M. Louis, R. Sethy, J. Kumar, S. Katao, R. Guillot, T. Nakashima, C. Allain, T. Kawai and R. Métivier, *Chem. Sci.*, 2019, **10**, 843–847.
142 S. Ito, R. Sekine, M. Munakata, M. Asami, T. Tachikawa, D. Kaji, K. Mishima and Y. Imai, *ChemPhotoChem*, 2021, **5**, 920–925.
143 S. L. Price, *Chem. Soc. Rev.*, 2014, **43**, 2098–2111.
144 C. Wang and C. C. Sun, *Mol. Pharmaceutics*, 2019, **16**, 1732–1741.
145 X. Feng, A. D. Becke and E. R. Johnson, *CrystEngComm*, 2021, **23**, 4264–4271.